

# Thermalization of a boost-invariant non-Abelian plasma: Holographic approach with boundary sourcing

---

## Loredana Bellantuono

*Dipartimento di Fisica, Università di Bari, via Orabona 4, I-70126 Bari, Italy*

*INFN, Sezione di Bari, via Orabona 4, I-70126 Bari, Italy*

*E-mail: [loredana.bellantuono@ba.infn.it](mailto:loredana.bellantuono@ba.infn.it)*

## Pietro Colangelo

*INFN, Sezione di Bari, via Orabona 4, I-70126 Bari, Italy*

*E-mail: [pietro.colangelo@ba.infn.it](mailto:pietro.colangelo@ba.infn.it)*

## Fulvia De Fazio\*

*INFN, Sezione di Bari,*

*via Orabona 4, I-70126 Bari, Italy*

*E-mail: [fulvia.defazio@ba.infn.it](mailto:fulvia.defazio@ba.infn.it)*

## Floriana Giannuzzi

*Dipartimento di Fisica, Università di Bari, via Orabona 4, I-70126 Bari, Italy*

*E-mail: [floriana.giannuzzi@ba.infn.it](mailto:floriana.giannuzzi@ba.infn.it)*

In a holographic approach, the evolution of a 4D strongly coupled non-Abelian plasma towards equilibrium can be studied investigating a 5D gravitational dual. The process driving the plasma out-of-equilibrium can be described by boundary sourcing, a deformation of the boundary metric; the analysis of the late-time dynamics allows to understand how the hydrodynamic regime settles in. We apply the method to a boost-invariant case, considering the effects of different quenches, solving the Einstein equations in the bulk and studying the time-dependence of observables such as the effective temperature, the energy density and the pressures. The main outcome is that, if the effective temperature of the system when the quench is switched off is  $T_{eff}(\tau^*) = 500$  MeV, thermalization is reached within a time of  $\mathcal{O}(1 \text{ fm}/c)$ , an important information if the case of the QCD plasma produced in relativistic heavy ion collisions is considered.

*The European Physical Society Conference on High Energy Physics*

*22–29 July 2015*

*Vienna, Austria*

---

\*Speaker.

## 1. Introduction

For strongly coupled fluids, as those produced in ultrarelativistic heavy ion collisions at RHIC and LHC, it is important to understand whether the late-time dynamics can be described by a low viscosity hydrodynamics, and what is the elapsed time needed to reach equilibrium after a perturbation. This requires studying the stress-energy tensor  $T_{\nu}^{\mu} \sim \text{diag}(-\varepsilon, p_{\perp}, p_{\perp}, p_{\parallel})$ , whose components are the system energy density  $\varepsilon$  and the pressures  $p_{\perp}, p_{\parallel}$  along one of the two transverse directions (with respect, e.g., to the heavy ion collision axis) and in the longitudinal direction. A framework to study the transient process from a far-from-equilibrium state is the holographic approach, based on the conjectured correspondence between a supersymmetric, conformal field theory defined in a four dimensional (4D) space-time and a gravity theory in a five dimensional Anti de-Sitter space (AdS<sub>5</sub>) times a five dimensional sphere S<sup>5</sup> [1]. The gauge theory is defined on the 4D boundary of AdS<sub>5</sub>. The connection has been extended to the nonlinear fluid dynamics [2,3]. Non-equilibrium can be studied solving the 5D Einstein bulk equations for the metric subject to suitable time-dependent boundary condition, and the boundary theory stress-energy tensor results from the holographic renormalization procedure [4].

To drive the system out-of-equilibrium within this framework, a distortion of the boundary metric due to external sources can be introduced [5]. Here we describe the analysis in [6], that goes further the proposal in [5] in two respects. First, various kinds of quenches are considered, to investigate whether and how the onset of the hydrodynamic regime is related to the distortion profiles. Moreover, an algorithm for the numerical solution of the Einstein equations has been developed, the details of which can be found in [6]. In the holographic framework, thermalization can also be studied starting from initial states characterized by an assigned energy density [7].

## 2. Boundary sourcing

As described in [5], the effect of a time-dependent deformation of the 4D boundary metric is the production of gravitational radiation propagating in the bulk, with the possible formation of a black hole. Hence, the study of the process towards equilibrium in the 4D theory can be afforded studying the time evolution of the 5D dual geometry. We choose 4D coordinates  $x^{\mu} = (x^0, x^1, x^2, x^3)$ , with  $x^3 = x_{\parallel}$  identified with the axis in the direction of collisions and along which the plasma expands. Boost-invariance along that axis is imposed, as well as translation invariance and  $O(2)$  rotational invariance in the  $x_{\perp} = \{x^1, x^2\}$  plane. In terms of the proper time  $\tau$  and rapidity  $y$ , with  $x^0 = \tau \cosh y$ ,  $x_{\parallel} = \tau \sinh y$ , the 4D Minkowski line element reads:  $ds_4^2 = -d\tau^2 + dx_{\perp}^2 + \tau^2 dy^2$ .

A way of distorting the boundary metric, leaving the spatial three-volume unvaried and respecting the chosen symmetries, is through a function  $\gamma(\tau)$ :

$$ds_4^2 = -d\tau^2 + e^{\gamma(\tau)} dx_{\perp}^2 + \tau^2 e^{-2\gamma(\tau)} dy^2 . \quad (2.1)$$

(2.1) can be viewed as the metric of the boundary of a 5D bulk in which the gravity dual is defined. Adopting Eddington-Finkelstein coordinates and denoting with  $r$  the fifth coordinate, the 5D bulk metric can be written as

$$ds_5^2 = 2drd\tau - Ad\tau^2 + \Sigma^2 e^B dx_{\perp}^2 + \Sigma^2 e^{-2B} dy^2 . \quad (2.2)$$

The boundary corresponds to  $r \rightarrow \infty$ . Due to the imposed symmetries, the metric functions  $A$ ,  $\Sigma$  and  $B$  depend on  $r$  and  $\tau$  only. Directional derivatives along the infalling radial null geodesics and the outgoing radial null geodesics can be defined,  $\xi' = \partial_r \xi$  and  $\dot{\xi} = \partial_\tau \xi + \frac{1}{2} A \partial_r \xi$ , for a generic function  $\xi(r, \tau)$ .

The 5D metric (2.2) solves Einstein equations with negative cosmological constant. In terms of  $A(r, \tau)$ ,  $\Sigma(r, \tau)$  and  $B(r, \tau)$  the equations can be cast in the form [5]:

$$\Sigma(\dot{\Sigma})' + 2\Sigma'\dot{\Sigma} - 2\Sigma^2 = 0 \quad (2.3)$$

$$\Sigma(\dot{B})' + \frac{3}{2}(\Sigma'\dot{B} + B'\dot{\Sigma}) = 0 \quad (2.4)$$

$$A'' + 3B'\dot{B} - 12\frac{\Sigma'\dot{\Sigma}}{\Sigma^2} + 4 = 0 \quad (2.5)$$

$$\ddot{\Sigma} + \frac{1}{2}(\dot{B}^2\Sigma - A'\dot{\Sigma}) = 0 \quad (2.6)$$

$$\Sigma'' + \frac{1}{2}B'^2\Sigma = 0. \quad (2.7)$$

The solutions are constrained to reproduce the 4D metric (2.1) for  $r \rightarrow \infty$ , hence

$$\frac{A(r, \tau) - r^2}{r} \xrightarrow[r \rightarrow \infty]{} 0, \quad \frac{\Sigma(r, \tau)}{r} \xrightarrow[r \rightarrow \infty]{} \tau^{\frac{1}{3}}, \quad B(r, \tau) \xrightarrow[r \rightarrow \infty]{} -\frac{2}{3} \log \tau + \gamma(\tau). \quad (2.8)$$

Moreover, if the distortion of the boundary metric starts at  $\tau = \tau_i$ , the metric functions at  $\tau_i$  must give the AdS<sub>5</sub> metric

$$ds_5^2 = 2drd\tau + r^2 \left[ -d\tau^2 + dx_\perp^2 + \left( \tau + \frac{1}{r} \right)^2 dy^2 \right], \quad (2.9)$$

hence initial conditions must be imposed,

$$A(r, \tau_i) = r^2, \quad \Sigma(r, \tau_i) = r \left( \tau_i + \frac{1}{r} \right)^{1/3}, \quad B(r, \tau_i) = -\frac{2}{3} \log \left( \tau_i + \frac{1}{r} \right). \quad (2.10)$$

Various profiles can be chosen for the deformation  $\gamma(\tau)$ , with different structures, duration and intensity. We generically define the profile

$$\gamma(\tau) = w \left[ \text{Tanh} \left( \frac{\tau - \tau_0}{\eta} \right) \right]^7 + \sum_{j=1}^N \gamma_j(\tau, \tau_{0,j}), \quad (2.11)$$

with

$$\gamma_j(\tau, \tau_{0,j}) = c_j f_j(\tau, \tau_{0,j})^6 e^{-1/f_j(\tau, \tau_{0,j})} \Theta \left( 1 - \frac{(\tau - \tau_{0,j})^2}{\Delta_j^2} \right), \quad f_j(\tau, \tau_{0,j}) = 1 - \frac{(\tau - \tau_{0,j})^2}{\Delta_j^2}. \quad (2.12)$$

This represents sequences of  $N$  "pulses", each one of intensity  $c_j$  and duration proportional to  $\Delta_j$ , with the possibility of superimposing a smooth deformation of intensity  $w$ . The response of the 5D bulk geometry to the quenches describes the way equilibration is achieved.

In [6] different models have been investigated, corresponding to different sets of parameters in Eqs. (2.11)-(2.12). We report the results of model  $\mathcal{A}$ , representing two pulses, with parameters

$w = 0$  and  $N = 2$ ,  $c_1 = 1$ ,  $\Delta_{1,2} = 1$ ,  $\tau_{0,1} = \frac{5}{4}\Delta_1$ ,  $c_2 = 2$ . Moreover, two different values of  $\tau_{0,2}$ :  $\tau_{0,2} = \frac{17}{4}\Delta_2$  and  $\tau_{0,2} = \frac{9}{4}\Delta_2$  are considered, varying the time elapsed between the pulses. The distortion ends at  $\tau_f^{\mathcal{A}} = 5.25$  and  $\tau_f^{\mathcal{B}} = 3.25$  for the two cases, respectively. Model  $\mathcal{C}$  is a sequence of pulses superimposed to a smooth distortion, and is obtained with

$$w = \frac{2}{5}, \quad \eta = 1.2, \quad \tau_0 = 0.25 \quad \Delta_j = 0.8 \quad (j = 1, 2, 3, 4), \quad c_{0,1} = 0.5, \quad c_{0,2} = 1, \quad c_{0,3} = 0.35, \\ c_{0,4} = 0.3, \quad \tau_{0,1} = \tau_0 + 1.5, \quad \tau_{0,2} = \tau_0 + 3.8, \quad \tau_{0,3} = \tau_0 + 6.1, \quad \tau_{0,4} = \tau_0 + 8.4.$$

In this case the last short pulse ends at  $\tau_f^{\mathcal{C}} = 9.45$ .

Black-brane solutions of the Einstein equations for the various models are found numerically [6], obtaining the apparent and the event horizon allowing to define the system effective temperature  $T_{eff}$ , together with  $\Sigma(r_h, \tau)^3$ , the area of each horizon per unit of rapidity. The components of the boundary stress-energy tensor are also obtained.

Assuming homogeneity, boost-invariance and invariance under rotations in the transverse plane with respect to the fluid velocity, the components of  $T_\mu^\nu$  only depend on the proper time  $\tau$  [8]. Moreover,  $T_\mu^\nu$  conserved and traceless implies that a single function  $f(\tau)$  is involved, so that one writes

$$T_\mu^\nu = \text{diag} \left( -f(\tau), f(\tau) + \frac{1}{2}\tau f'(\tau), f(\tau) + \frac{1}{2}\tau f'(\tau), -f(\tau) - \tau f'(\tau) \right). \quad (2.13)$$

For a perfect fluid, the equation of state  $\varepsilon = 3p$ , with  $p = p_\parallel = p_\perp$ , fixes the  $\tau$  dependence:  $\varepsilon(\tau) = \frac{\text{const}}{\tau^{4/3}}$ , while viscous effects produce a deviation of  $f(\tau)$  [9]. An effective temperature  $T_{eff}(\tau)$  can be defined through the relation  $\varepsilon(\tau) = \frac{3}{4}\pi^4 T_{eff}(\tau)^4$ . The calculation in  $\mathcal{N} = 4$  SYM gives the asymptotic  $\tau$  dependence [10]:

$$T_{eff}(\tau) = \frac{\Lambda}{(\Lambda\tau)^{1/3}} \left[ 1 - \frac{1}{6\pi(\Lambda\tau)^{2/3}} + \frac{-1 + \log 2}{36\pi^2(\Lambda\tau)^{4/3}} \right. \\ \left. + \frac{-21 + 2\pi^2 + 51 \log 2 - 24(\log 2)^2}{1944\pi^3(\Lambda\tau)^2} + \mathcal{O} \left( \frac{1}{(\Lambda\tau)^{8/3}} \right) \right], \quad (2.14)$$

corresponding, for the energy density, the pressure ratio and anisotropy, to

$$\varepsilon(\tau) = \frac{3\pi^4\Lambda^4}{4(\Lambda\tau)^{4/3}} \left[ 1 - \frac{2c_1}{(\Lambda\tau)^{2/3}} + \frac{c_2}{(\Lambda\tau)^{4/3}} + \mathcal{O} \left( \frac{1}{(\Lambda\tau)^2} \right) \right] \quad (2.15)$$

$$\frac{p_\parallel}{p_\perp} = 1 - \frac{6c_1}{(\Lambda\tau)^{2/3}} + \frac{6c_2}{(\Lambda\tau)^{4/3}} + \mathcal{O} \left( \frac{1}{(\Lambda\tau)^2} \right), \quad (2.16)$$

$$\frac{\Delta p}{\varepsilon} = \frac{p_\perp - p_\parallel}{\varepsilon} = 2 \left[ \frac{c_1}{(\Lambda\tau)^{2/3}} + \frac{2c_1^2 - c_2}{(\Lambda\tau)^{4/3}} + \mathcal{O} \left( \frac{1}{(\Lambda\tau)^2} \right) \right] \quad (2.17)$$

( $c_1 = \frac{1}{3\pi}$  and  $c_2 = \frac{1 + 2\log 2}{18\pi^2}$ ). The parameter  $\Lambda$  depends on the model for quenches.

### 3. Results

Although we discuss here the results of models  $\mathcal{A}$  and  $\mathcal{C}$ , all the considered models share common features, namely the formation of a horizon and the evolution towards the hydrodynamic

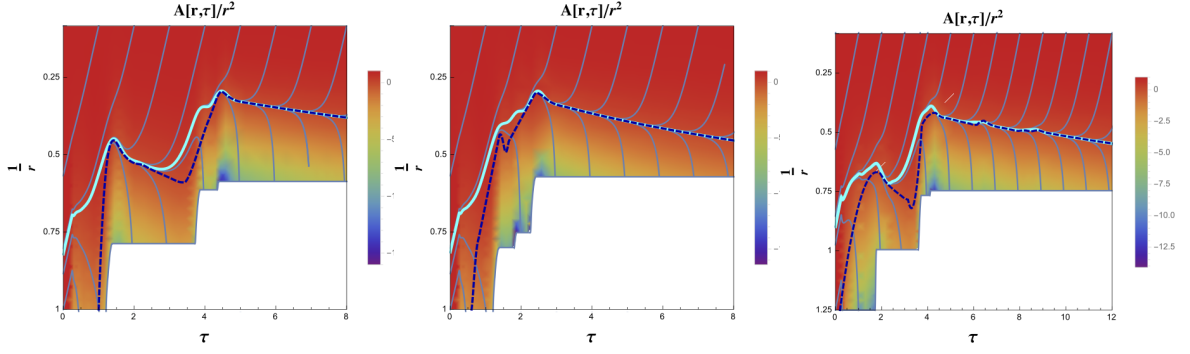


**Figure 1:** The panels show the function  $A(r, \tau)/r^2$  vs  $\tau$  and  $1/r$ , obtained solving the Einstein equations in the case of the model  $\mathcal{A}$  of two distant (left) or close pulses (central panel) in the boundary metric, and of the model  $\mathcal{C}$  (right panel). The color bars indicate the values of the function. The gray lines are radial null outgoing geodesics, the dashed dark blue line is the apparent horizon, the continuous cyan line is the event horizon. The excision in the low- $r$  region used in the calculation is shown.

regime [6]. Such evolution has different features for the various observables. The effective temperature and the energy density start evolving according to their hydrodynamic expression immediately after the quench is switched off. On other hand, pressures take longer to reach the hydrodynamic regime: a "thermalization time"  $\tau_p$  can be defined from the condition

$$\left| \frac{p_{\parallel}(\tau_p)/p_{\perp}(\tau_p) - (p_{\parallel}(\tau_p)/p_{\perp}(\tau_p))_H}{p_{\parallel}(\tau_p)/p_{\perp}(\tau_p)} \right| = 0.05, \quad (3.1)$$

where  $(p_{\parallel}(\tau_p)/p_{\perp}(\tau_p))_H$  is given by (2.16).

In the case of model  $\mathcal{A}$ , for two distant pulses the horizon forms in a two-step process in which the sequence of the boundary distortion is followed, as shown in Fig. 1 (left panel) which displays the metric function  $A(r, \tau)/r^2$ , together with the apparent and event horizons. The temperature, reported in Fig. 2, has two decreasing regimes, each one after each of the two pulses, with the relaxation of the system starting immediately after the end of each perturbation. The same can be noticed looking at the area of the apparent horizon per unit of rapidity,  $\Sigma(r_h, \tau)^3$ , which reaches a constant value, soon after the pulses. On such time scales, the behaviour of the components of  $T_V^\mu$  shows no isotropization after the first pulse.

For two nearly overlapping quenches, no structure is observed before the end of the perturbation. The horizon area per unit of rapidity sharply increases during the distortion, reaching the asymptotic large  $\tau$  value  $\Sigma(r_h, \tau)^3 = \pi^3 \Lambda^2$  soon after the end of the distortion.

The time  $\tau^*$  at which energy density  $\varepsilon(\tau^*)$  differs from the hydrodynamic value  $\varepsilon_H(\tau^*)$  in (2.15) by less than 5% essentially coincides with the end of the perturbation, while the time defined in (3.1) is larger. The difference  $\tau_p - \tau^*$  measures the elapsed time between the end of the quench and the restoration of the hydrodynamical regime. It can be expressed in physical units introducing a scale in the system by imposing  $T_{eff}(\tau^*) = 500$  MeV. The time scales and the values of the parameter  $\Lambda$  are collected in Table 1. The difference  $\tau_p - \tau^*$  is found to be order (or less than) 1 fm/c, an important information for the strongly coupled QCD plasma. This result favourably compares with QCD-based models [11].

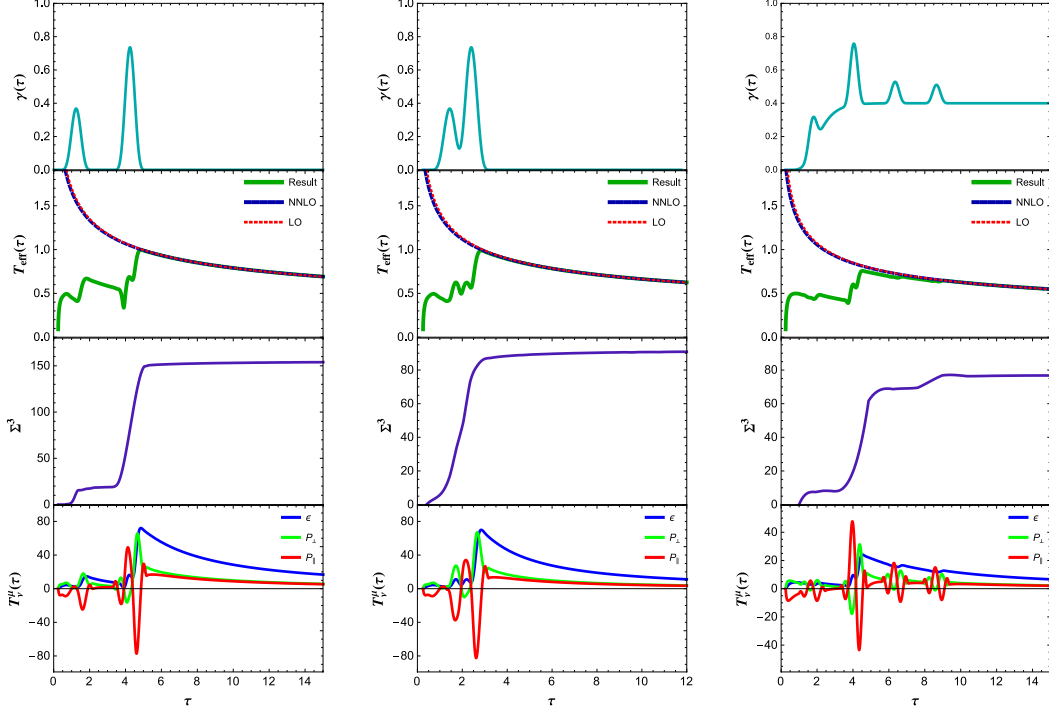


**Figure 2:** For three different quench profiles (models  $\mathcal{A}$  and  $\mathcal{C}$ ) the panels show (from top to bottom) the profile  $\gamma(\tau)$ , the temperature  $T_{eff}(\tau)$ , the horizon area  $\Sigma^3(r_h, \tau)$  per unit of rapidity, and the three components  $\varepsilon(\tau)$ ,  $p_{\perp}(\tau)$  and  $p_{\parallel}(\tau)$  of the stress-energy tensor  $T_v^{\mu}$ .

model	$\tau^*$	$\tau_p$	$\Lambda$	$\Delta\tau = \tau_p - \tau^*$ (fm/c)
$\mathcal{A}$ (1)	5.25	6.8	2.25	0.60
$\mathcal{A}$ (2)	3.25	6.0	1.73	1.03
$\mathcal{C}$	9.45	10.24	1.59	0.20

**Table 1:** Results for different models of boundary quenches.

## 4. Conclusions

Through distortions of the boundary metric, in a boost-invariant setup and using holography, it is possible to describe relaxation of an out-of-equilibrium strongly coupled fluid. Independently of the considered deformation, we have found that a horizon forms in the bulk metric, and an effective  $\tau$ -dependent temperature can be defined.  $T_{eff}(\tau)$  evolves according to a viscous hydrodynamic expression as soon as the quench is switched off, while the pressures have an elapsed time (setting  $T_{eff}(\tau^*) = 500$  MeV) of a fraction of fm/c before the hydrodynamic regime is reached.

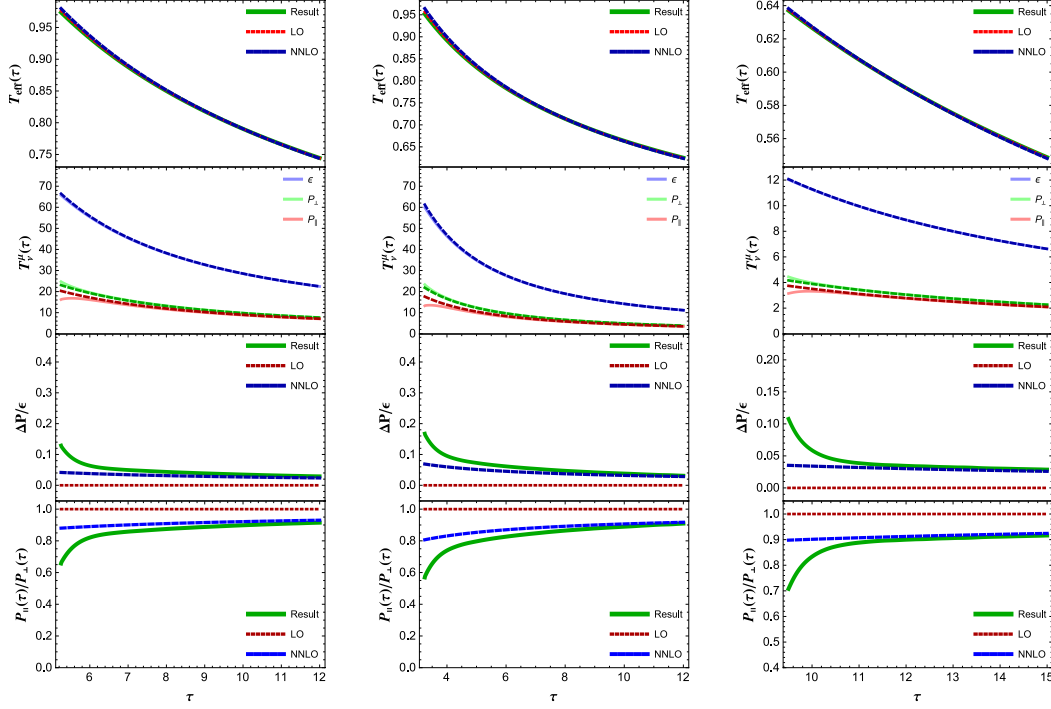


**Figure 3:** For three different quench profiles (models  $\mathcal{A}$  and  $\mathcal{C}$ ) the panels show, from top to bottom: temperature  $T_{eff}(\tau)$ , components  $\epsilon(\tau)$ ,  $p_{\perp}(\tau)$  and  $p_{\parallel}(\tau)$  of the stress-energy tensor, pressure anisotropy  $\Delta p/\epsilon = (p_{\perp} - p_{\parallel})/\epsilon$  and ratio  $p_{\parallel}/p_{\perp}$ , computed for  $\tau > \tau_f^{\mathcal{A},\mathcal{C}}$ . The short and long dashed lines correspond to the hydrodynamic result and to the NNLO result in the  $1/\tau$  expansion.

## References

- [1] J. M. Maldacena,  
*The Large N limit of superconformal field theories and supergravity.*  
*Int.J.Theor.Phys.* **38** (1999) 1113–1133
- [2] S. Bhattacharyya, V. E. Hubeny, S. Minwalla, and M. Rangamani.  
*Nonlinear Fluid Dynamics from Gravity.*  
*JHEP* **0802** (2008) 045
- [3] J. Casalderrey-Solana, H. Liu, D. Mateos, K. Rajagopal, and U. A. Wiedemann.  
*Gauge/String Duality, Hot QCD and Heavy Ion Collisions.*  
arXiv:1101.0618
- [4] S. de Haro, S. N. Solodukhin, and K. Skenderis.  
*Holographic reconstruction of space-time and renormalization in the AdS / CFT correspondence.*  
*Commun.Math.Phys.* **217** (2001) 595
- [5] P. M. Chesler and L. G. Yaffe.  
*Horizon formation and far-from-equilibrium isotropization in supersymmetric Yang-Mills plasma.*  
*Phys.Rev.Lett.* **102** (2009) 211601  
P. M. Chesler and L. G. Yaffe.

- Boost invariant flow, black hole formation, and far-from-equilibrium dynamics in  $N = 4$  supersymmetric Yang-Mills theory.*  
*Phys.Rev.* **D82** (2010) 026006.
- [6] L. Bellantuono, P. Colangelo, F. De Fazio and F. Giannuzzi.  
*On thermalization of a boost-invariant non-Abelian plasma.*  
*JHEP* **07** (2015) 053
- [7] M. P. Heller, R. A. Janik, and P. Witaszczyk.  
*A numerical relativity approach to the initial value problem in asymptotically Anti-de Sitter spacetime for plasma thermalization - an ADM formulation.*  
*Phys.Rev.* **D85** (2012) 126002  
M. P. Heller, D. Mateos, W. van der Schee and M. Triana.  
*Holographic isotropization linearized.*  
*JHEP* **1309**, 026 (2013)  
J. Jankowski, G. Plewa and M. Spalinski.  
*Statistics of thermalization in Bjorken Flow,*  
*JHEP* **1412**, 105 (2014)
- [8] J. Bjorken.  
*Highly Relativistic Nucleus-Nucleus Collisions: The Central Rapidity Region.*  
*Phys.Rev.* **D27** (1983) 140
- [9] R. A. Janik and R. B. Peschanski.  
*Asymptotic perfect fluid dynamics as a consequence of AdS/CFT.*  
*Phys.Rev.* **D73** (2006) 045013
- [10] M. P. Heller and R. A. Janik.  
*Viscous hydrodynamics relaxation time from AdS/CFT.*  
*Phys.Rev.* **D76** (2007) 025027  
R. Baier, P. Romatschke, D. T. Son, A. O. Starinets, and M. A. Stephanov.  
*Relativistic viscous hydrodynamics, conformal invariance, and holography.*  
*JHEP* **0804** (2008) 100
- [11] M. Ruggieri, A. Puglisi, L. Oliva, S. Plumari, F. Scardina and V. Greco.  
*Thermalization and Isotropization of Color-Electric Flux Tubes.*  
arXiv:1505.08081 [hep-ph]